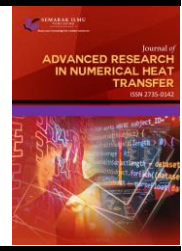




## Journal of Advanced Research in Numerical Heat Transfer

Journal homepage:  
<https://semarakilmu.com.my/journals/index.php/arnht/index>  
ISSN: 2735-0142



# Modelling of the Flame Synthesis of Single-walled Carbon Nanotubes in Non-premixed Flames with Aerosol Catalyst

Muhammad Syafiq Ridhwan Selamat<sup>1</sup>, Muhammad Thalhah Zainal<sup>1</sup>, Mohd Fairus Mohd Yasin<sup>1,\*</sup>, Norikhwan Hamzah<sup>1</sup>, Nor Azwadi Che Sidik<sup>2</sup>

<sup>1</sup> High Speed Reacting Flow Laboratory (HIREF), School of Mechanical Engineering, Faculty of Engineering, Universiti Teknologi Malaysia, 81310 Johor Bahru, Johor, Malaysia

<sup>2</sup> Malaysia-Japan International Institute of Technology (MJIT), UTM Kuala Lumpur, Jalan Sultan Yahya Petra, Kuala Lumpur, Malaysia

### ARTICLE INFO

#### Article history:

Received 9 March 2023

Received in revised form 14 April 2023

Accepted 10 May 2023

Available online 30 June 2023

#### Keywords:

Flame synthesis; Single-walled carbon nanotube (SWCNT); Discrete particle modelling (DPM); Multi-scale model

### ABSTRACT

The use of aerosol catalyst in the flame synthesis of carbon nanotube (CNT) is known to yield single-walled CNT (SWCNT) that is useful for various applications. Modelling works are needed to optimize operating conditions for SWCNT growth but are unavailable. Therefore, a baseline model for the aerosol-catalyst system in flames is developed and the effect of oxygen on SWCNT growth is investigated. A baseline flame model for a normal diffusion flame with 24% oxygen concentration at the inlet is established via Computational Fluid Dynamic simulation. A dispersed phase model (DPM) is employed to simulate the entrainment of catalyst particles. The flame model is coupled with a published CNT growth rate model to predict the CNT growth rate at each particle. Inlet oxygen concentration is varied from 19% to 27% to study the effect of oxygen on SWCNT growth. Satisfactory validation of the baseline flame shape and temperature is established. Results show that particle 3 for the baseline case yields the highest CNT length compared to other particles due to the suitable path for the synthesis. The particles are classified based on the shortest time residence, moderate and longest time residence. Increasing oxygen concentration from 19% to 27% results in a 30% decrease in CNT length for particle 3 for each inlet condition due to lower carbon precursor and composition in the flame. Furthermore, the results showed that regardless of burner operating conditions, high SWCNT growth is consistently predicted between 120-140 mm HAB, which indicates the existence of an optimum range of species concentration for SWCNT growth in aerosol-based flame synthesis. Thus, it can be inferred that SWCNT growth in the aerosol-based method is highly dependent on carbon source and moderately dependent on temperature.

## 1. Introduction

Since the discovery of carbon nano-structure materials, countless research has been carried out to explore and optimize the production of carbon nanotube (CNT) [1,2]. CNT have superior thermal and mechanical properties compared to other materials. The quality of CNTs depend on the CNT morphology which are often classified into single-walled carbon nanotubes (SWCNT) and multi-wall

\* Corresponding author.

E-mail address: [mohdfairus@mail.fkm.utm.my](mailto:mohdfairus@mail.fkm.utm.my) (Mohd Fairus Mohd Yasin)

<https://doi.org/10.37934/arnht.13.1.3951>

carbon nanotubes (MWCNT). SWCNT possesses better electrical, mechanical, and thermal properties compared to MWCNT and is more desired in electronics-based applications [3]. The common methods used to synthesize SWCNT are the catalytic chemical vapor deposition (CCVD), arc discharge, laser ablation and flame synthesis. The flame synthesis method is more energy-efficient and cost-effective compared to the rest of the synthesis methods.

There are two common methods of introducing catalyst as the CNT growth site in flame, which are the substrate-based and aerosol-based methods. The growth period of the latter is in the order of milliseconds while the former may reach up several minutes. Furthermore, the aerosol method provides a continuous supply of catalysts and thus continuous growth, which is favorable for mass production [4]. Recent study by Okada and co-worker, they proposed flame assist chemical vapor deposition (FACVD) to get benefit from both methods. The study implements floating type catalyst to produce CNT. The FACVD, has proven to produce high quality SWCNT with average diameter of 0.96nm, a small diameter deviation which is 0.21nm and approximately 90wt% high carbon purity [5]. There are a few reports exploring the catalyst floating strategy, concentrating mainly on the low-pressure environment. Diener *et al.*, [6] did CNT synthesis at 10 kPa using different fuels ( $C_2H_2$ ,  $C_2H_4$  and  $C_6H_6$ ) and metallocene (Fe, Ni and Co) as catalyst.  $C_2H_2$  and  $C_2H_4$  were more preferred than  $C_6H_6$  for high-quality CNT production. However, systematic modelling study for aerosol-based catalyst in flame synthesis is scarce.

Previous experimental study by Vander Wal and Hall [7] employed a premixed flame with fuel mixture of  $CO/H_2/He$  to synthesize SWCNT. In the study, iron particles were deployed as catalyst and were introduced into the flame using the aerosol method. Another experimental study by Unrau *et al.*, [8] showed that SWCNT growth was more favorable at higher oxygen concentration in an inverse diffusion flame setup with aerosol-based iron oxide catalyst. Vander Wal *et al.*, [9] conducted detailed studies of CNTs synthesis in premixed hydrocarbon flame. In their studies, a McKenna burner was used with a stainless-steel chimney at the top of the central fuel tube to stabilize the pyrolysis steam and collect the CNT. Various hydrocarbon fuels with different metallic additives were tested at varying equivalence ratios [9]. A CFD simulation was performed in a study by Endo and co-workers to determine critical parameters for the growth rate of CNT such as temperature, velocity, and concentration of species [10]. The study revealed a linear increase in the growth rate of CNT with an improvement in fuel concentration. In the research by Wen *et al.*, [11], CHEMKIN models a premixed methane-oxygen-argon flame to obtain temperature distribution, species concentration, and time of residence of the catalyst. In order to estimate the number of carbon atoms adsorbed on the catalyst particle surface, the numerical findings were then treated as an input for the particle scale model. Another research provided a CFD flame model to predict flame temperature and distribution of carbon precursor where concentration was put as a predictor of growth site in flame on the catalyst particle trajectory [12]. In the absence of CNT growth simulation, the expected catalyst trajectories inside the flame were used to estimate the particle residence time [12]. The UNICORN combustion code was used by Naha *et al.*, [13] to measure species concentration and temperature in a diffusion flame environment at various HABs that are used as feedback in the growth rate model. The authors have compared the expected deposition rate and surface density of carbon atoms on the surface of the catalyst with those of the CVD measurement experimental [3].

The change in  $z_{st}$  influenced by oxygen concentration, fuel concentration, and fuel type affects CNT growth in diffusion flame though systematic study on  $z_{st}$  effects are limited by the experimental conditions. For example, the works of Unrau and co-workers show that increase of oxygen content to as high as 45% and 75% results in flame with large  $z_{st}$  of approximately 0.7. High  $z_{st}$  indicated by high oxygen content and diluted fuel were found to be favorable for CNT growth where the authors pointed out the competition with soot and PAH particles was avoided [14]. The effect of oxygen

concentration on CNT growth has been investigated by Hou and co-workers using a counterflow flame and an inverse diffusion flame [15,16]. In particular, both studies demonstrate that the oxygen composition influences the formation of different morphologies. For instance, at low oxygen content of 21% O<sub>2</sub>, only CNTs are formed whereas at higher oxygen content of 50% O<sub>2</sub>, carbon nano-onions are synthesized. The experimental work of Hou *et al.*, [16] measured CNT growth region in inverse diffusion flame using substrate-based catalyst at varying inlet conditions including at varying O<sub>2</sub> concentration. The study showed that as O<sub>2</sub> increased from 25% to 40%, a slight increase in growth region size is observed. However, the trend of improved CNT at higher O<sub>2</sub> cannot be concretely concluded as the growth region across varying O<sub>2</sub> are measured at different HAB. Recent study by Hamzah *et al.*, [17] showed that an 8% increase in oxygen concentration at the inlet results in the decrease of growth region axial extent by 82% with a 35% reduction in the amorphous carbon layer thickness (ACLT). In the study, nickel wire was employed as the substrate. A previous modelling study demonstrated that the increase in the inlet oxygen concentration of rich inverse diffusion flame resulted in a significant increase in the flame temperature with minimal change in carbon source concentration to allow the expansion of growth region [18].

From the brief literature above, it is evident that predictive numerical study on aerosol-based synthesis in flame and the associated burner operating conditions is not widely studied due to high temporal and spatial resolution of the flame parameters will allow detailed study on the growth of CNT with aerosol catalyst. The same study is impossible to be done in the experiment due to the limitation of the measurement resolution. Therefore, the objective of the present paper is to develop a baseline model for flame synthesis based on aerosol catalyst and to investigate the effect of oxidizer concentration on the SWCNT growth.

## 2. Methodology

In the present study, a diffusion flame model with aerosol catalyst entrainment is developed using the CFD software Fluent Ansys version 2019 R3 based on the normal diffusion flame in Zainal [3]. The flame shape is validated against the actual flame with and without the inclusion of wire mesh substrate at 10 mm height above the burner (HAB) via inspection of the flame height whereas the temperature validation is done via comparison between predicted and measured radial temperature at 13 mm HAB. Once validation is completed, the DPM model is employed to analyze the CNT growth rate on a catalyst particle along a streamline. To simplify the modelling work and reduce the computational time, the actual burner geometry is simplified into a two-dimensional axisymmetric domain, as shown in Figure 1.

The CFD solver used to model the diffusion flame is a pressure-based and density-based flamelet solver. The influence of gravity is considered due to the significant effect on the flame simulation. The  $k-\epsilon$  turbulence model and the P-1 radiation model deployed to account for local turbulence and heat loss through radiation, respectively. The basic governing equations for CFD solver include the continuity equation and the momentum transport equation. All second order upwind discretization scheme is employed except for the gradient parameter that use green-gauss cell-based discretization.

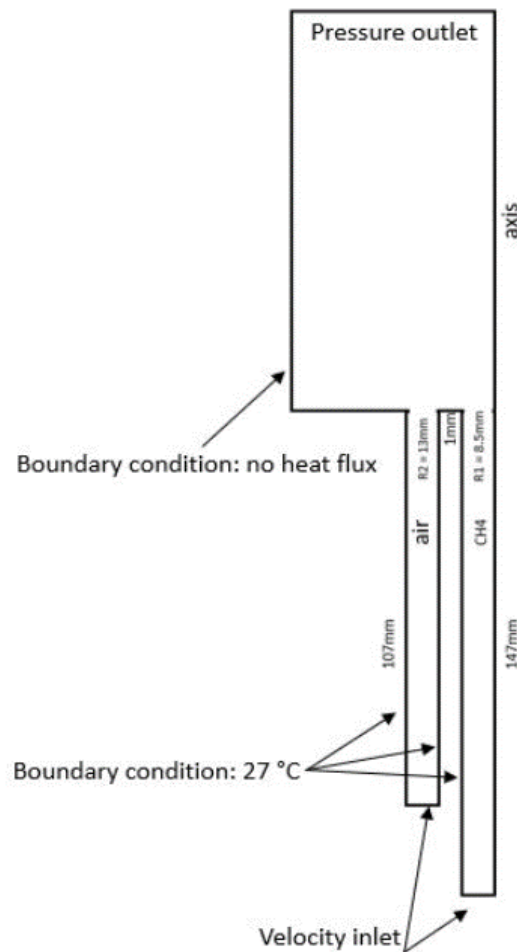


**Fig. 1.** Flame model geometry

The boundary condition for the oxidizer and fuel concentration as shown in Table 1 and Table 2 below. Note that the Flame ID convention of the previous study that the present study is based on is retained for ease of referencing [18]. Two flame configurations are considered for flame validation, which are Flame3B at 10 and 13 mm HAB and Flame3CW. The difference in  $z_{st}$  and global equivalence ratio is expected from the varying fuel and oxidizer composition. The mesh independence test is achieved at 70,000 cells. Disperse phase model (DPM) is applied to simulate entrainment of catalyst particles into the combustion region and to analyze the path of the particles from the oxidizer inlet to the outlet. The DPM model is set up so that the particles interact with the reacting flow in continuous phase to supply continuous particle analysis in the domain. The DPM source setting is updated every 10-flow interaction. The catalyst injection properties are shown in Table 3 below.

**Table 1**  
 Flame configuration and validation conditions

| Flame ID  | Fuel component (%vol) |          | Oxidizer component (%vol) |          | Global equivalence ratio | $Z_{st}$ |
|-----------|-----------------------|----------|---------------------------|----------|--------------------------|----------|
|           | Methane               | Nitrogen | Oxygen                    | Nitrogen |                          |          |
| Flame 3AW | 50                    | 50       | 19                        | 81       | 0.584                    | 0.13     |
| Flame 3BW | 50                    | 50       | 21                        | 79       | 0.53                     | 0.14     |
| Flame 3CW | 50                    | 50       | 24                        | 76       | 0.465                    | 0.15     |
| Flame 3DW | 50                    | 50       | 27                        | 73       | 0.415                    | 0.16     |

| Validation conditions | Fuel component (%vol) |          | Oxidizer component (%vol) |          | Global equivalence ratio | $Z_{st}$ |
|-----------------------|-----------------------|----------|---------------------------|----------|--------------------------|----------|
|                       | Methane               | Nitrogen | Oxygen                    | Nitrogen |                          |          |
| Flame 3B<br>10HAB     | 100                   | 0        | 21                        | 79       | 1.055                    | 0.055    |
| Flame 3B<br>13HAB     | 100                   | 0        | 21                        | 79       | 1.055                    | 0.055    |
| Flame 3CW             | 50                    | 50       | 24                        | 76       | 0.465                    | 0.15     |

**Table 2**  
 Standing flame inlet condition

|                           | Fuel inlet | Oxidizer inlet |
|---------------------------|------------|----------------|
| Mass flow rate (kg/s)     | 4.45e-6    | 7e-5           |
| Turbulent intensity (%)   | 5          | 5              |
| Hydraulic diameter (m)    | 0.018      | 0.024          |
| Temperature (K)           | 300        | 300            |
| Mean mixture fraction     | 1          | 0              |
| Mixture fraction variance | 0          | 0              |

**Table 3**  
 DPM setting for simulating aerosol catalyst entrainment

| Injection type         | Surface                      |
|------------------------|------------------------------|
| Release surface        | Air inlet                    |
| Particle type          | Inert gas-no vaporization    |
| Particle material      | Nickel with uniform diameter |
| Velocity x/y direction | OFF                          |
| Catalyst diameter      | 50 nanometers                |
| Temperature            | 300K                         |
| Total flow rate        | 1e-20 kg/s                   |
| Physical models        | Spherical                    |
| Particle rotation      | OFF                          |
| Turbulent dispersion   | Discrete random walk model   |
| Number of tries        | 1                            |

### 3. Results

#### 3.1 Baseline Flame Validation

In the present flame validation, Flame3B with the presence of wire mesh is chosen as the baseline flame in temperature and shape validation. The Flame3CW without the presence of wire mesh is chosen as baseline flame for current standing flame. The operating condition of the baseline case employed for validation is shown in Table 1. Validation of the flame shape is done based on comparison of the flame sheet between the predicted and actual flame image. The  $Z_{st}$  isoline at 0.055 from model contour is compared with the actual flame image at 10 mm HAB as shown in Figure 2.

The predicted flame shape is observed to resemble closely the experimental flame model, indicating a reasonable prediction of the flame. Furthermore, the predicted temperature contour shifts from hot to cooler region towards the centreline, which mimics the hot outer blue surface and the cooler orange chemiluminescence in the inner region of the actual flame. The flame shape comparison for Flame3CW without the presence of mesh is shown in Figure 3. Similar to the predicted flame shape under wire mesh, the predicted blue flame of the standing flame version of Flame3CW appears slightly the same height as the actual flame, which indicate reasonable prediction accuracy of the flame model.

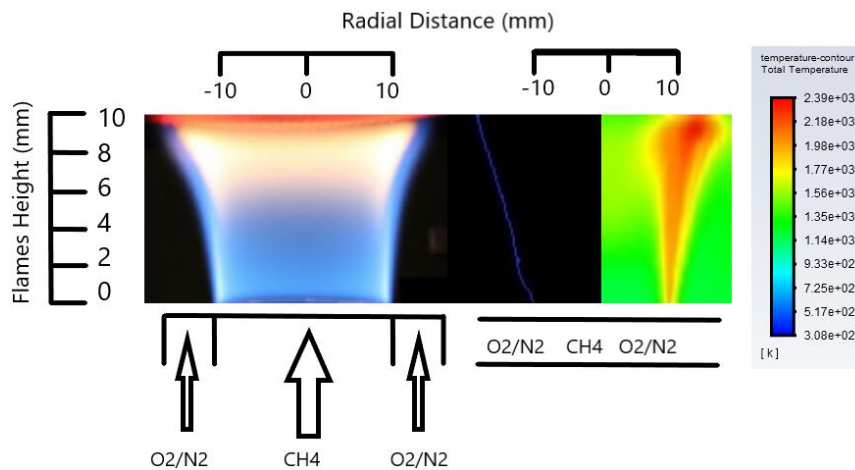


**Fig. 2.** Flame shape predicted based on  $z_{st}$  isoline with the value of 0.055 (middle panel) and temperature contour (right panel) compared to the actual experimental flame (left panel)

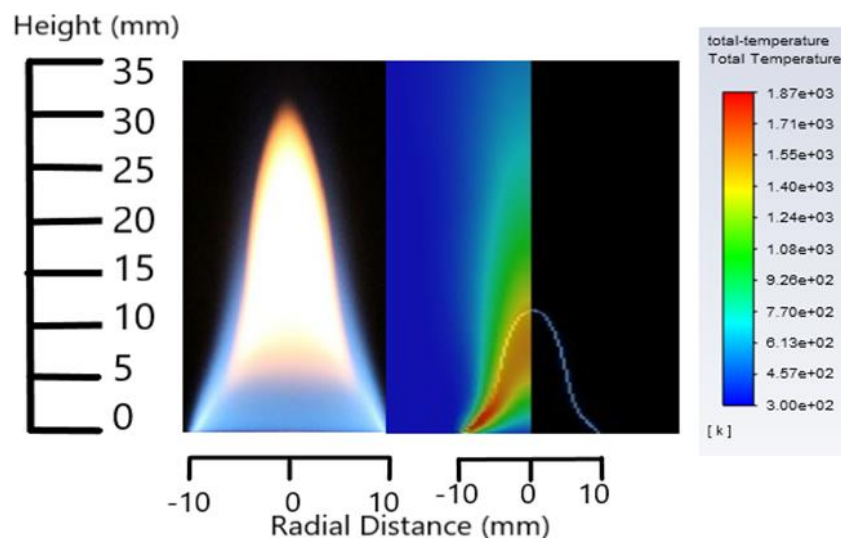


**Fig. 3.** Flame shape predicted based on  $z_{st}$  isoline with the value of 0.055 (middle panel) and temperature contour (right panel) compared to the actual experimental flame (left panel)

### 3.2 Discrete Particle Modelling of CNT Growth in Aerosol Catalyst

The purpose of the DPM simulation is to mimic the entrainment of aerosol catalyst particles, which serves as the growth site for SWCNT in flame. The DPM allows the movement of the particle to be tracked with Lagrangian method. Based on the location of the particle where the CFD results

were extracted, the temperature, species composition, and the residence time for the particle are extracted. The CFD result obtained from DPM simulation is used to plot temperature of the catalyst against residence time as shown in Figure 4. A total of 30 particles are released from the oxidizer inlet. The particle is arranged with random spacing in between other particles to simulate actual particle movement in experimental. Three particles with the highest, lowest, and moderate residence time, which are represented by particle 2, 3, and 20, respectively are chosen for analysis. The said particles were chosen based on consistent streamline movement across all flame under study. Nonetheless a random motion is applied in the DPM setting to closely resemble actual particle motion, though such setting resulted in different streamlines. Particles other than the ones mentioned earlier are less feasible for analysis due to their highly random motion and displacement in an irrelevant pattern. Results for CNT growth for the particles are analyzed at varying HAB and residence time. All particles are employed for the baseline case for standing flame which is Flame3CW with 24% oxygen concentration.

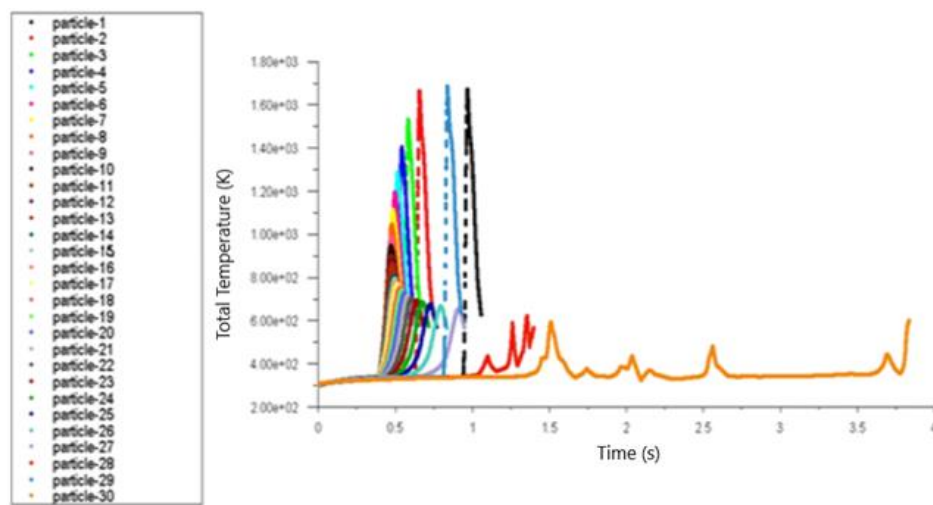


**Fig. 4.** Temperature vs time for 30 particles

Figure 5 to Figure 7 show the flame structure and CNT length plot with respect to residence time and HAB for particles 2, 3, and 20 for Flame3CW with 24% of oxygen without the present of wire mesh. The flame structure of the standing flame starts from 0 mm to 100 mm HAB, which is the upstream section before the burner exit whereas the HAB from, 100 mm to 200 mm is the main combustion region. The horizontal line in the length plot in Figure 5 to Figure 7 is the threshold line for effective high CNT growth, which is taken to be 70% of the maximum CNT length to be consistent with previous study [19]. The intercept of the threshold and the CNT length plot defines the boundaries of CNT growth region in the physical space.

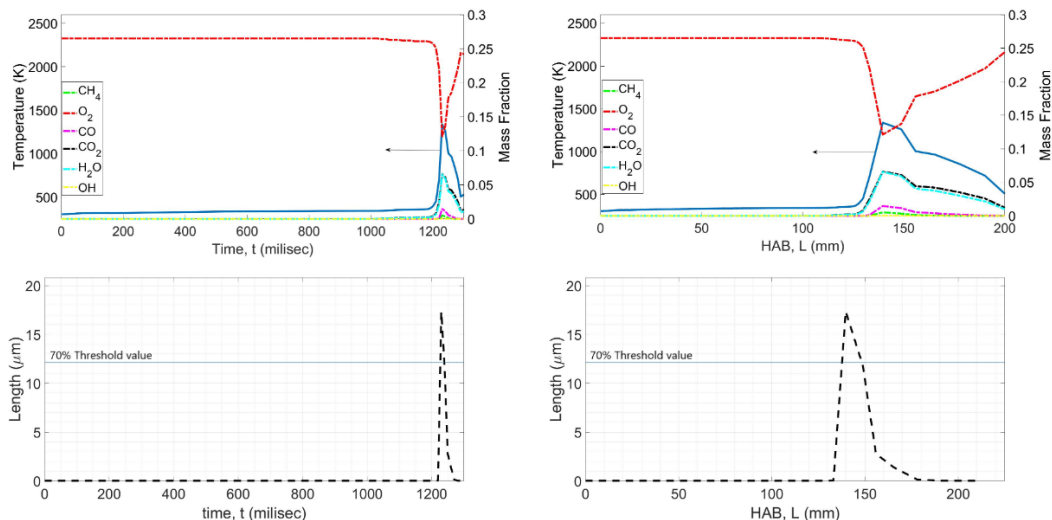


**Fig. 5.** Flame structure (top) and CNT length plot (bottom) at varying exposure time and HAB for particle 2 in Flame3CW

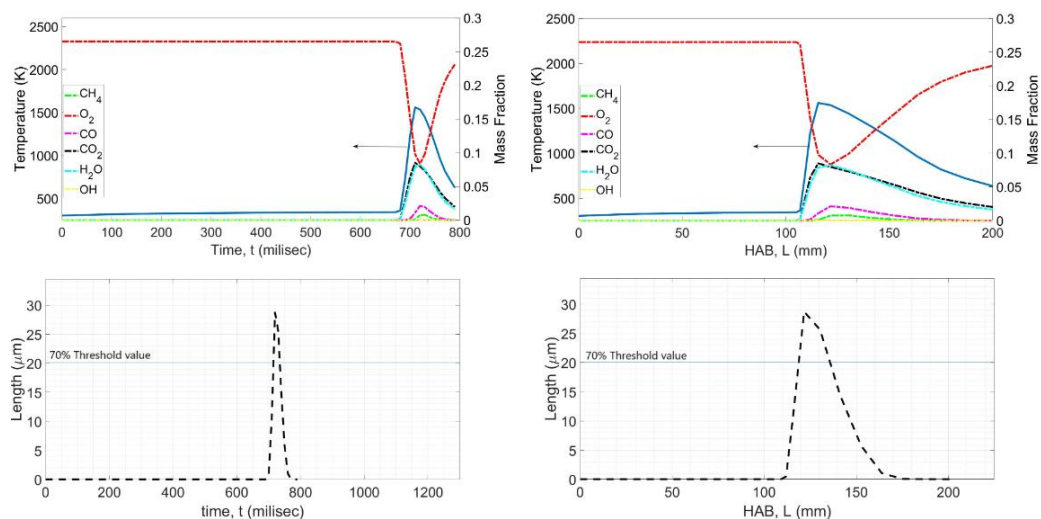


**Fig. 6.** Flame structure (top) and CNT length plot (bottom) at varying exposure time and HAB for particle 3 in Flame3CW

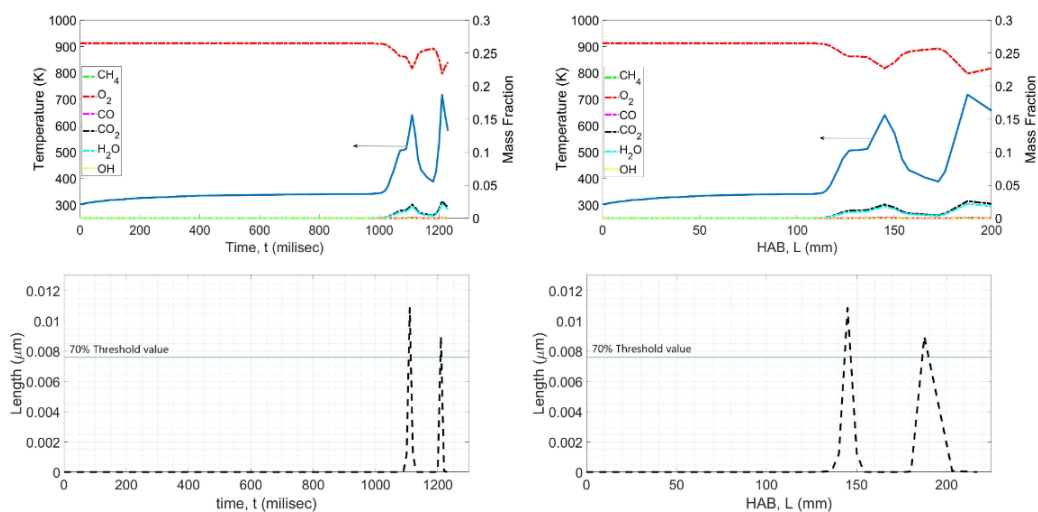


**Fig. 7.** Flame structure (top) and CNT length plot (bottom) at varying exposure time and HAB for particle 20 in Flame3CW

The species concentration for all particles are the same, but the particle streamlines, and exposure time is different. Figure 7 shows that the smallest CNT length is produced by particle 20. However, CNT growth at particle 20 happens at later time at approximately 1200 milliseconds compared to growth at particles 2 and 3. Furthermore, occurrence of CNT growth at particle 20 happens twice as indicated by the double peaks of the CNT length plot due to the particles entering the flame and exit it twice. The CNT length produced by particle 3 is the highest compared to the rest with a maximum length of 28 micrometer. Based on the comparison of CNT growth in Figure 5 to Figure 7, particle 3 is chosen for further analysis at varying burner inlet condition where the respective streamline yield the most significant effect compared to the exposure time of the particles.

The flame structure is applied to all cases in present study from Flame3AW to Flame3DW. Figure 8 to Figure 10 show the result of CNT at varying oxygen concentration for particle 3 without the wire mesh. For Flame3AW with 19% oxygen concentration, the result showed that the predicted CNT length can reach up to 30 micrometers which is slightly higher than that of Flame3CW with 24% oxygen concentration. A more noticeable change is the growth area that slightly widens compared to Flame3CW with 24% oxygen concentration. The flame structure plot in Figure 8 represents the thermochemical profile of particle 3 in Flame3AW. The corresponding length plot shows that CNT start to grow at 560 millisecond which corresponds to a flame location of 113 mm HAB. The particle achieves maximum temperature of approximately 1500 K at 600 milliseconds that corresponds to 120 mm HAB where the predicted CNT length is 30 micrometers. Based on Figure 8, the lower oxygen concentration than is expected for Flame3AW with 19% oxygen. Chemical reaction occurs after 107 mm HAB which is slightly above the burner inlet.

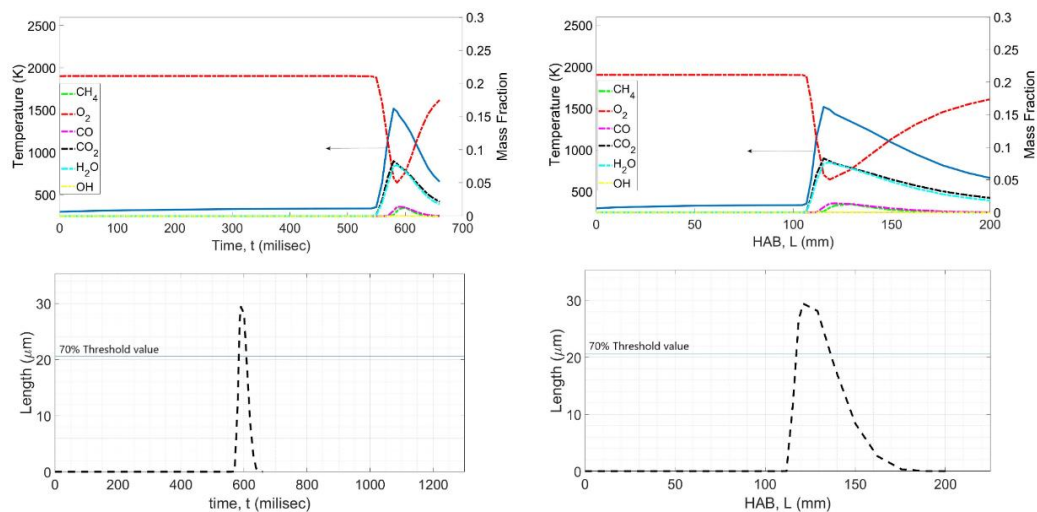


**Fig. 8.** Flame structure (top) and CNT length plot (bottom) at varying exposure time and HAB for particle 3 in Flame3AW

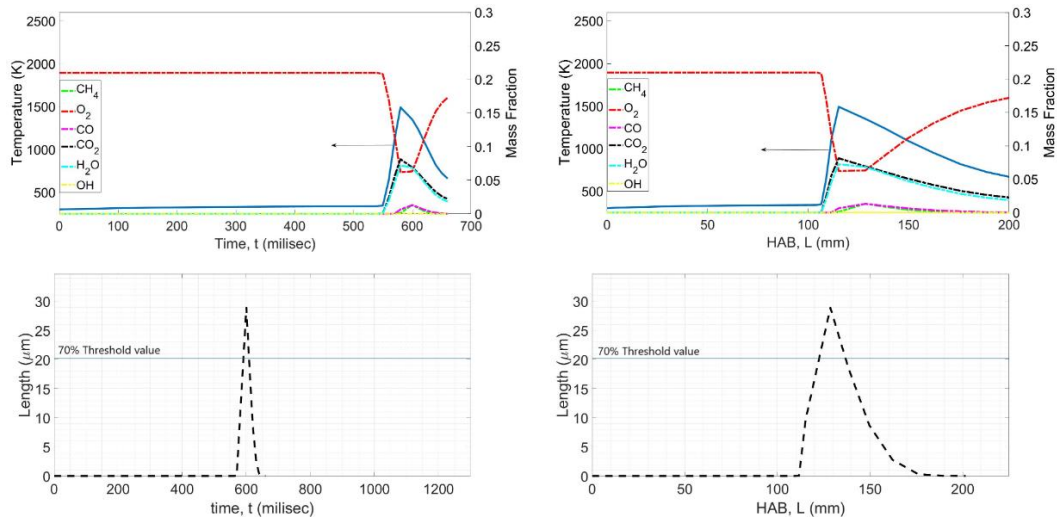


**Fig. 9.** Flame structure (top) and CNT length plot (bottom) at varying exposure time and HAB for particle 3 in Flame3BW

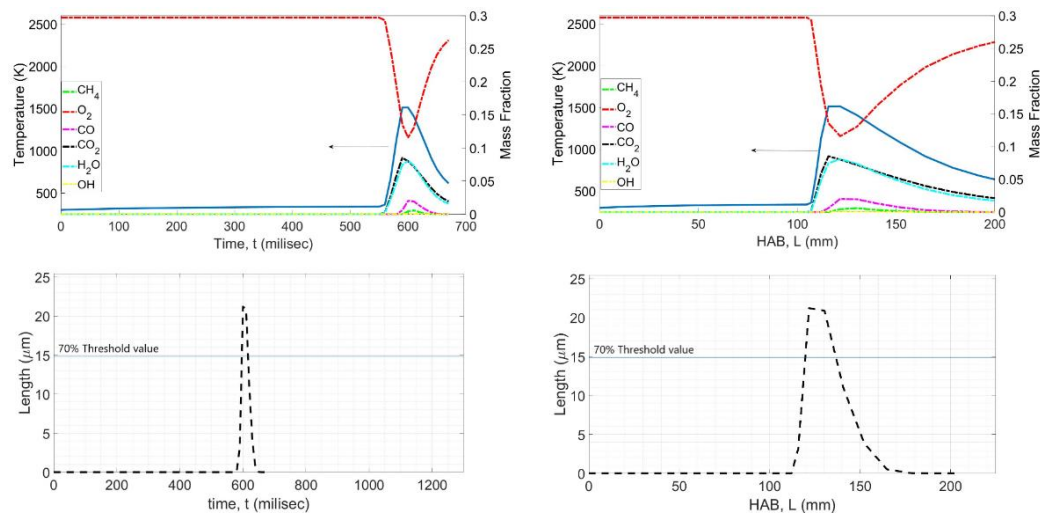


**Fig. 10.** Flame structure (top) and CNT length plot (bottom) at varying exposure time and HAB for particle 3 in Flame3DW

The flame structure plot in Figure 9 shows the thermochemical profile for particle 3 in Flame3BW with 21% oxygen. CNT start to grow at 560 millisecond which corresponds to 113 mm HAB. The particle achieves maximum temperature at 580 milliseconds which is approximately 1500 K. The oxygen concentration starts to decrease at 550 milliseconds with the other species concentration increases respectively. The decrease of oxygen and increase of combustion product species indicate occurrence of combustion. For the said flame operating conditions, the predicted CNT length is 29 micrometers at 600 milliseconds corresponding to 130 mm HAB. For the final case of Flame3DW with 27% oxygen concentration, the result predicted CNT length of about 21 micrometers is much lower compared to other cases as shown in Figure 10. The CNT start to grow at 580 millisecond which is at 112 mm HAB. The particle achieves high temperature at 580 milliseconds which is approximately 1600 K. The predicted CNT length is 21 micrometers at 600 milliseconds at 120 mm HAB. A drop in magnitude of the predicted CNT length from 30micrometers to 20micrometers as the oxygen concentration is increased from 19 to 27% shows that the CNT predicted length decreases with an increase in the oxidizer concentration.

The observations from Figure 5 to Figure 10 are summarized in Table 4. The physics of the flame is well captured at increasing O<sub>2</sub> where the flame temperature is expected to increase due to abundance of hot combustion region from the excess O<sub>2</sub> [3,19]. However, the overall, maximum CNT length, showed a reduction of about 30% at increasing oxygen concentration from 19% to 27% O<sub>2</sub>. Although the oxygen plot in the flame structures indicated by the red plot correctly illustrated increasing of oxygen concentration from Flame3AW to 3DW, the major carbon source CH<sub>4</sub> indicated by the green plot showed more than 75% drop from approximately 0.04 to less than 0.01, which explains the reduction in maximum CNT length at higher oxygen concentration. On the other hand, the temperature increases of about 6% from the case of 19% O<sub>2</sub> (Flame3AW) to 27% O<sub>2</sub> (Flame3DW) does not significantly affect the CNT growth despite the growth rate model's ability to respond to temperature and carbon source concentration [20]. Thus, it can be inferred that SWCNT growth in the aerosol-based method is highly dependent on carbon source and moderately dependent on temperature.

Although the literature highlights the positive influence of oxygen on CNT growth, the same observation is not produced in the present study which can be attributed to the random location of particle 3 that potentially fell in a less favorable thermochemical environment within the flame during the simulation [17]. Nonetheless, the results interestingly show that regardless of inlet condition, a consistent optimum HAB for SWCNT growth from 120 to 140 mm HAB is achieved as indicated by the left and right boundaries of high SWCNT growth region. This finding suggests that there exists an optimum height for SWCNT grow occur in aerosol-based flame synthesis.

**Table 4**  
Growth region summary

| Flame ID  | Growth region range (mmHAB) | Start growth (mmHAB) | Stop growth (mmHAB) | Maximum Temperature (K) | Maximum CNT length (μm) |
|-----------|-----------------------------|----------------------|---------------------|-------------------------|-------------------------|
| Flame 3AW | 120-140                     | 113                  | 180                 | 1500                    | 30                      |
| Flame 3BW | 122-136                     | 113                  | 175                 | 1500                    | 29                      |
| Flame 3CW | 118-135                     | 112                  | 170                 | 1600                    | 28                      |
| Flame 3DW | 117-134                     | 112                  | 165                 | 1600                    | 21                      |

#### 4. Conclusions

In conclusion, a baseline multi-scale model was established for flame synthesis with aerosol-based catalyst with an emphasis on SWCNT growth. Validation work is carried out with reasonable comparison of the flame shape and radial temperature for the bell-shaped and standing flame variants of the normal diffusion flame under study. DPM simulation was employed to show SWCNT growth on aerosol-based catalyst particles entrained into the flame via the oxidizer inlet. Out of the 30 particles released into the simulation domain, 3 were chosen for analysis in the baseline case based on short, moderate, and long residence time. Particle 3 with long residence time is found to exhibit the best SWCNT growth among the three particles and is chosen for analysis for effect of varying O<sub>2</sub> on SWCNT growth. The results show that at high oxidizer concentration, short CNT length is produced, due to the drop in carbon precursor concentration and the unfavorable thermochemical environment within the location of the particle. The results also showed that high growth of SWCNT is consistently predicted at HAB of approximately 120-140 mm, which indicate an optimum range of HAB for SWCNT growth in aerosol-based synthesis.

## Acknowledgement

This research was funded by Universiti Teknologi Malaysia through UTM Fundamental Research grant (UTMFR:PY/2019/01657) with cost centre number J130000.2551.21H10 and the Fundamental Research Grant Scheme (FRGS/1/2020/TK0/UTM/02/54) with cost number J130000.7851.5F377 and (FRGS/1/2019/TK05/UTM/02/8) with cost centre numbers R.J130000.7851.5F182 awarded by the Malaysian Ministry of Education.

## References

- [1] Iijima, Sumio. "Helical microtubules of graphitic carbon." *Nature* 354, no. 6348 (1991): 56-58. <https://doi.org/10.1038/354056a0>
- [2] Kroto, Harold W., James R. Heath, Sean C. O'Brien, Robert F. Curl, and Richard E. Smalley. "C<sub>60</sub>: Buckminsterfullerene." *Nature* 318, no. 6042 (1985): 162-163. <https://doi.org/10.1038/318162a0>
- [3] Zainal, Muhammad Thalhah. "Modelling the flame synthesis of carbon nanotube (cnt) in inverse diffusion flame." *Master's thesis, Universiti Teknologi Malaysia* (2017).
- [4] Hamzah, N., M. F. Mohd Yasin, M. Z. Mohd Yusop, A. Saat, and N. A. Mohd Subha. "Rapid production of carbon nanotubes: A review on advancement in growth control and morphology manipulations of flame synthesis." *Journal of Materials Chemistry A* 5, no. 48 (2017): 25144-25170. <https://doi.org/10.1039/C7TA08668G>
- [5] Okada, Shohei, Hisashi Sugime, Kei Hasegawa, Toshio Osawa, Shohei Kataoka, Hiroki Sugiura, and Suguru Noda. "Flame-assisted chemical vapor deposition for continuous gas-phase synthesis of 1-nm-diameter single-wall carbon nanotubes." *Carbon* 138 (2018): 1-7. <https://doi.org/10.1016/j.carbon.2018.05.060>
- [6] Diener, Michael D., Noah Nicholson, and John M. Alford. "Synthesis of single-walled carbon nanotubes in flames." *The Journal of Physical Chemistry B* 104, no. 41 (2000): 9615-9620. <https://doi.org/10.1021/jp001233f>
- [7] Vander Wal, Randall L., and Lee J. Hall. "Ferrocene as a precursor reagent for metal-catalyzed carbon nanotubes: competing effects." *Combustion and Flame* 130, no. 1-2 (2002): 27-36. [https://doi.org/10.1016/S0010-2180\(02\)00358-9](https://doi.org/10.1016/S0010-2180(02)00358-9)
- [8] Unrau, Chad J., Richard L. Axelbaum, and Phil Fraundorf. "Single-walled carbon nanotube formation on iron oxide catalysts in diffusion flames." *Journal of Nanoparticle Research* 12 (2010): 2125-2133. <https://doi.org/10.1007/s11051-009-9771-2>
- [9] Vander Wal, Randy L., Gordon M. Berger, and Lee J. Hall. "Single-walled carbon nanotube synthesis via a multi-stage flame configuration." *The Journal of Physical Chemistry B* 106, no. 14 (2002): 3564-3567. <https://doi.org/10.1021/jp012844g>
- [10] Endo, Hajime, Kazunori Kuwana, Kozo Saito, Dali Qian, Rodney Andrews, and Eric A. Grulke. "CFD prediction of carbon nanotube production rate in a CVD reactor." *Chemical Physics Letters* 387, no. 4-6 (2004): 307-311. <https://doi.org/10.1016/j.cplett.2004.01.124>
- [11] Wen, John Z., Matthew Celnik, Henning Richter, Meri Treska, John B. Vander Sande, and Markus Kraft. "Modelling study of single walled carbon nanotube formation in a premixed flame." *Journal of Materials Chemistry* 18, no. 13 (2008): 1582-1591. <https://doi.org/10.1039/b717256g>
- [12] Unrau, C. J., V. R. Katta, and R. L. Axelbaum. "Characterization of diffusion flames for synthesis of single-walled carbon nanotubes." *Combustion and Flame* 157, no. 9 (2010): 1643-1648. <https://doi.org/10.1016/j.combustflame.2010.05.005>
- [13] Naha, Sayangdev, Swarnendu Sen, Anindya K. De, and Ishwar K. Puri. "A detailed model for the flame synthesis of carbon nanotubes and nanofibers." *Proceedings of the Combustion Institute* 31, no. 2 (2007): 1821-1829. <https://doi.org/10.1016/j.proci.2006.07.224>
- [14] Unrau, C. J., R. L. Axelbaum, P. Biswas, and P. Fraundorf. "Synthesis of single-walled carbon nanotubes in oxy-fuel inverse diffusion flames with online diagnostics." *Proceedings of the Combustion Institute* 31, no. 2 (2007): 1865-1872. <https://doi.org/10.1016/j.proci.2006.08.009>
- [15] Hou, Shuhn-Shyurng, Wei-Cheng Huang, and Ta-Hui Lin. "Flame synthesis of carbon nanostructures using mixed fuel in oxygen-enriched environment." *Journal of Nanoparticle Research* 14 (2012): 1-11. <https://doi.org/10.1007/s11051-012-1243-4>
- [16] Hou, Shuhn-Shyurng, De-Hua Chung, and Ta-Hui Lin. "High-yield synthesis of carbon nano-onions in counterflow diffusion flames." *Carbon* 47, no. 4 (2009): 938-947. <https://doi.org/10.1016/j.carbon.2008.11.054>
- [17] Hamzah, Norikhwan, Mohd Fairus Mohd Yasin, Mohd Zamri Mohd Yusop, Muhammad Aniq Shazni Mohammad Haniff, Mohd Faizal Hasan, Khairul Fikri Tamrin, and Nurul Adilla Mohd Subha. "Effect of fuel and oxygen concentration toward catalyst encapsulation in water-assisted flame synthesis of carbon nanotubes." *Combustion and Flame* 220 (2020): 272-287. <https://doi.org/10.1016/j.combustflame.2020.07.007>

- [18] Hamzah, N., M. F. Mohd Yasin, M. Z. Mohd Yusop, A. Saat, and N. A. Mohd Subha. "Growth region characterization of carbon nanotubes synthesis in heterogeneous flame environment with wire-based macro-image analysis." *Diamond and Related Materials* 99 (2019): 107500. <https://doi.org/10.1016/j.diamond.2019.107500>
- [19] Zainal, Muhammad Thalhah, Mohd Fairus Mohd Yasin, Muhammad Abid Ira Irawan, Muhammad Faizullizam Roslan, Norikhwan Hamzah, and Mohd Zamri Mohd Yusop. "Investigation on the deactivation of cobalt and iron catalysts in catalytic growth of carbon nanotube using a growth rate model." *Journal of Advanced Research in Materials Science* 51, no. 1 (2018): 11-22.
- [20] Zainal, M. T., MF Mohd Yasin, and M. Abdul Wahid. "Investigation of the coupled effects of temperature and partial pressure on catalytic growth of carbon nanotubes using a modified growth rate model." *Materials Research Express* 3, no. 10 (2016): 105040. <https://doi.org/10.1088/2053-1591/3/10/105040>